



Effects of the morphology of sediment-transporting channels on the erosion and deposition of debris flows

Songtang He^{1,2,3} · Daojie Wang^{1,2} · Shiqiu Chang^{1,2,3} · Yingchao Fang^{1,2,3} · Huijuan Lan^{1,2,3}

Received: 2 January 2018 / Accepted: 14 July 2018 / Published online: 24 July 2018
© Springer-Verlag GmbH Germany, part of Springer Nature 2018

Abstract

A series experiments are conducted to investigate the effects of streambed profile on the erosion and deposition of debris flows. It is found that straight channel can increase the run out of debris flows by 10–25%, compared to that of surfaces without channels, and that travel distance was positively correlated with the hydraulic radius of the channel. In addition, the presence of straight channels caused the volume of debris flow deposition to become normally distributed with respect to travel distance. In the case of curved channels, increases in the sinuosity index resulted in significant blockage and obstruction. In the deposition zone, the maximum deposition volume for a channel with a comparatively low sinuosity index (1.05) was < 50% of the minimum deposition volume for a straight channel. Furthermore, the channel curvature affected not only the positions of deposition peaks along the travel distance but also the debris flow magnitudes in each unit interval (0.5 m). This study demonstrates the effects of differences in channel morphology on the erosional and depositional processes of gully debris flows. These findings are of significant importance for guiding debris flow risk assessment and for the restoration and reconstruction of downstream regions.

Keywords Debris flows · Channel morphology · Hydraulic radius · Sinuosity index · Jiangjia gully

Introduction

Gully erosion, as the main source of river sediment and a way of soil erosion, has gradually become a hot topic in geosciences in recent years, and has been widely concerned by scholars from all over the world (Zhu 2012; Dotterweich et al. 2012; Xiong et al. 2010). They all sensed that gully erosion was a significant issue for mountain security and earth surface (Rozos et al. 2013), and should pay more attention to and continue studying the gully erosion, especially in ecologically fragile area (Lan et al. 2004).

In many minor watersheds, debris flows may dramatically alter the morphology of streambed profile when large quantities of debris are transported via debris flows from upstream to downstream regions, and finally result in the formation of gully with different depth and size. The cross section of gully are usually “U” type (Kirkby and Bracken 2009). In the case of larger scale debris flows, during the gradual transformation of viscous debris flows into diluted debris flows, erosion will occur in local sections of the gully bed, such that narrow channels may be formed in the deposits of earlier viscous debris flows (tiny “U”-shaped channels on the bottom of a large pre-existing “U”-shaped

✉ Daojie Wang
wangdj@imde.ac.cn

Songtang He
hst1529568372@126.com

Shiqiu Chang
shiqiu7@163.com

Yingchao Fang
1176988203@qq.com

Huijuan Lan
2692332976@qq.com

¹ Key Laboratory of Mountain Hazards and Earth Surface Processes, Chinese Academy of Sciences, Chengdu 610041, China

² Institute of Mountain Hazards and Environment, Chinese Academy of Sciences, #.9, Block4, Renminnanlu Road, Chengdu 610041, China

³ University of Chinese Academy of Sciences, 100049 Beijing, China

channel), resulting in the formation of compound sections in the gully bed (You and Cheng 2005). Gully erosion often accelerates the degradation process of soil because of its rapid and large amount of erosion. Data collected in different parts of the world show that soil loss rates by gully erosion represent from minimal 10% up to 94% of total sediment yield caused by water erosion (Jing 1986; Poesen et al. 2003). It can be seen that the gully on the streambed has a great influence on the movement of the debris flow in the valley (Benda 1990; Wells et al. 2009; Rengers and Tucker 2014, 2015).

In the past, most of scientists focused on the types and development stages of gully (Bocco 1991), and with the deepening of research, more and more researchers have begun to study the factors affecting the development of gully (e.g., cut rill) (Vandekerckhove et al. 2000; Morgan and Mngomezulu 2003; Carnicelli et al. 2009; Capra et al. 2009), and discussed the development of gully from the aspects of topography (Li et al. 2015), rainfall, soil properties, and human activities (Patton and Schumm 1975; Prosser 1996; Valentin et al. 2005; Vanwalleghem et al. 2005). To the best of our knowledge, under the condition of the same fluid characteristics, the higher the slope is, the larger the runoff is (Pan et al. 2012), and rainfall determines the transport characteristics of debris flow, according to statistical data (Adhikari and Koshimizu 2005; Gregoretti and Fontana 2008; Wenske et al. 2012). Little attention is paid to the impact of mature gullies [generally are not changed channels, also named permanent gully (Soil Science Society of America 2001)] on sediment transport. In particular, studies on the feedback mechanism between the channel morphologies and the erosional/depositional processes are currently very scarce (Bridge 2003; Liu et al. 2009; Cannon et al. 2010). The morphological features of the channel here include only its own shape (e.g., length, width, height, and bending), not the site conditions (e.g., slope, elevation difference) (Catani et al. 2005; Lee and Pradhan 2007; Tiranti et al. 2008; Tunusluoglu et al. 2008). However, in the field trip, we found that the morphology of mature gully has a significant influence on the movement of debris flow in the debris flow area. Such as based on field observation data on the Jiangjia gully (China) that were collected over a number of years, the obtained sinuosity index of the gully channels was fitted to the average depth of the deposits. The resulting fit at $R^2 = 0.73$ (Chang 2016) indicates that there is a certain level of positive correlation between the sinuosity index of the channels and the deposits of debris flows. In terms of the prominent debris flow zones, like the Jiangjia gully (where debris flows occur frequently), has shown a marked decrease in the occurrence of large debris flows in recent years, how the influence of the pre-existing channel on the runoff, speed and the erosion and siltation of debris flow is worth studying.

The purpose of this paper is to explore and elucidate the effects of different channel morphologies on the movements of debris flows (erosion and deposition), as well as the effects on depositions in alluvial fan regions through flume experiment. This study takes a non-dynamic approach (Major 1997; Li et al. 2004) to analyzing the geometrical state of deposits and erosional. In addition, our findings give people a warning that the impacts of channels on debris flows should not be overlooked and our findings are highly significant for disaster prevention and mitigation works on debris flows.

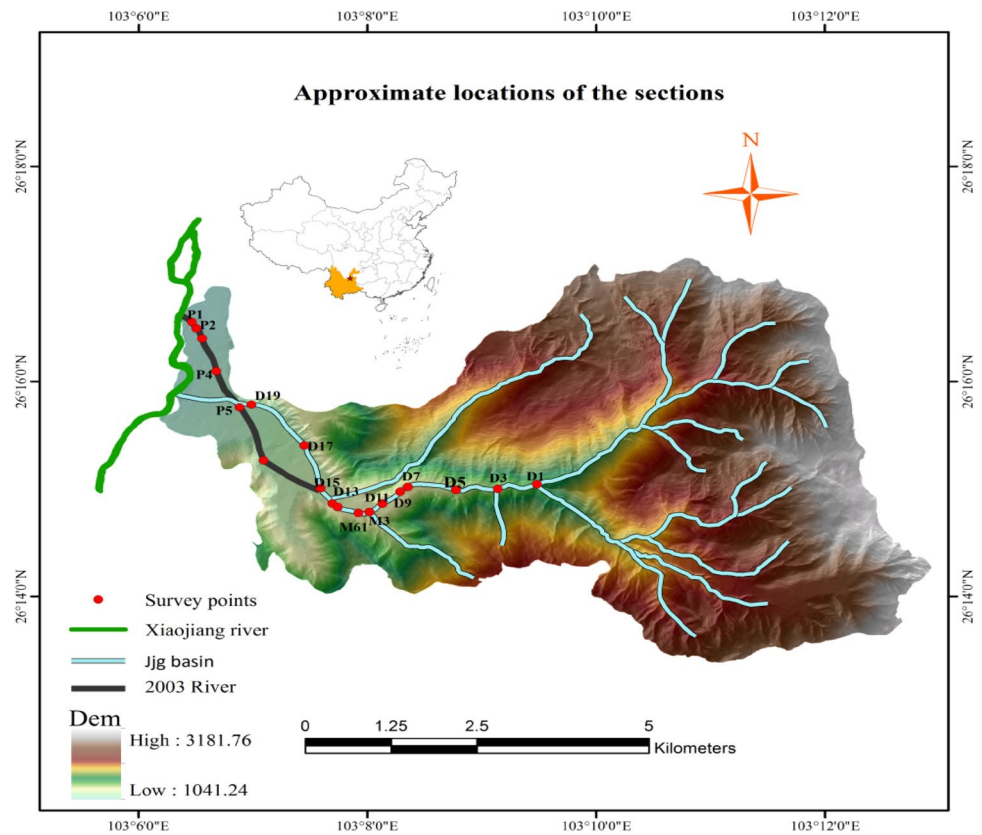
Research methodology and data processing

Study area

The Jiangjia gully is located in northeastern Yunnan Province ($26^{\circ}13' - 26^{\circ}17'N$, $103^{\circ}06' - 103^{\circ}13'E$) on the Xiaojiang fault zone in the eastern part of the Xikang–Yunnan Axis (where Precambrian metamorphic rock is exposed between Kangding and Yunnan Red River, China), which is characterized by highly complex tectonic structures, active tectonic movements, and intense seismic activity. The Jiangjia gully is mainly composed of slate (a kind of metamorphic rock) and sandstone, which are lithologically weak and easily weathered into thin sheets or flakes. Highly fragile rocks, frequent precipitation by southwest monsoon winds, and uncontrolled human economic activities (agriculture, mining, industry, etc.) all contribute to the occurrence of extremely well-developed debris flows in this region (Wu et al. 1990; He et al. 2016). Among the numerous gullies known for debris flows in Xiaojiang, Yunnan Province, the Jiangjia gully is where debris flows are largest in scale, occur most frequently, and pose the greatest threat to human lives and properties (Li et al. 1979). For these reason, the Jiangjia gully is nicknamed ‘the museum of debris flows’ (Hong et al. 2015).

This study took the segment of the gully that starts from the intersection of the Menqian gully and the Duo Zhao gully (D1) and extends to the confluence of the Jiangjia gully with the Xiaojiang River (P1) (Fig. 1) as the simulated area. The 14 observation sections along the Jiangjia gully can be grouped into three segments according to the position and width of each section as follows: (1) sections that are upstream of the debris flow observation station, including D1, D3, D5, D7, D9, and D11 (henceforth referred to as D1–D11), which are constrained by the distance between the mountains on either side and have widths ranging from 200 to 300 m; (2) sections between the debris flow observation station and the downstream debris flow drainage channel, including M3, M61, D13, and D15 (henceforth referred to as M3–D15), where the distance between the

Fig. 1 Locations of the studied gully sections within the Jiangjia gully basin (Jjg basin). ‘2003 river’ refers to the drainage channel constructed in 2003



two mountains increases and causes the section to widen rapidly, resulting in widths between 300 and 400 m; and (3) sections downstream of the debris flow drainage channels, including P4, P5, PL1, and PL2 (henceforth referred to as P4–PL2) are restricted by the man-made drainage channels constructed along both shores and consequently have widths < 100 m. These three segments form the circulation zone of the Jiangjia gully, which in recent years has shown the following characteristics: (1) the river bed is mostly covered by debris flow deposits; (2) distinct channels are observed in the river bed, which is bordered on either side by the foothills of the mountains; and (3) water/water–sand flows erode the gully along these channels, causing the river bed to gradually widen. As the mountains are composed mainly of mechanically weak and easily weathered phyllite and slate, the effects of erosion on the width of the riverbed are even more significant. The underlying surface has been severely eroded, resulting in crisscrossing incised gully throughout the channels (Fig. 2). Field data for these segments of the gully, obtained between 1957 and 2002, show intense sedimentation and the section with the highest sedimentation rate is located at the entrance of the Daaози gully (M3), where the 45-year sediment vertical accretion is approximately 45.6 m, with a average deposition rate of 1 m/year (He 2003). In addition, observations for the D7 section from 2003 to 2014 (Fig. 3) indicate that the changes that occurred

in this section were mainly due to deposition. However, a more detailed analysis of the sedimentation over time reveals that the sediments did not accumulate linearly but fluctuated periodically. This indicates that debris flow erosion and deposition in the Jiangjia gully are dynamically changing processes.

The field observations show that in recent years, debris flows that usually occur during the rainy season (June–October) have rarely reached the regions downstream of the man-made discharge channel (D15). One likely reason for this is that the run out are gradually decreasing (related to the reducing of the loose substance). A second possible cause is that the erosion and deposition processes, over many years, have created channels with different shapes on the underlying surface of the circulation zone, which have significantly altered the debris flow drainage (Fig. 2). Substantial lateral erosion exists in the foothills of the mountains, and portions of the debris flows that have insufficient momentum simply cease flowing and deposit sediment within the channels.

Experimental method and materials

From July to September 2015, the Dongchuan debris flow observation station of the Chinese Academy of Sciences performed a model-simulation experiment with an experimental apparatus composed of four parts, as shown in

Fig. 2 Various channel morphologies with different channel depths, widths, and lengths in the Jiangjia gully. The channels in **a–c** are deeper and more regular than those in **d**. Thus, they increase the runout of debris flow

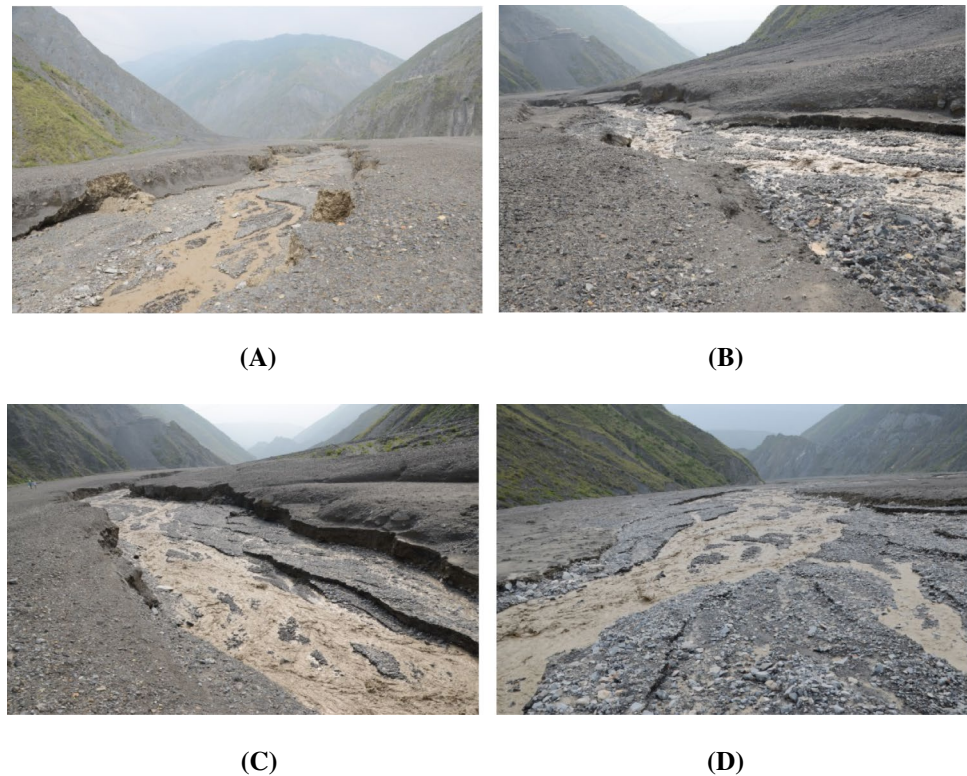


Fig. 3 Changes in average sedimentation over time. Here, the beginning of the sample code in the *x*-axis indicates the rank of the sample within the sample year (e.g., 2003-1 is the first sample for 2003), and the end of the code indicates the sample day within the sample year (e.g., 08/05 was sampled on August 5)

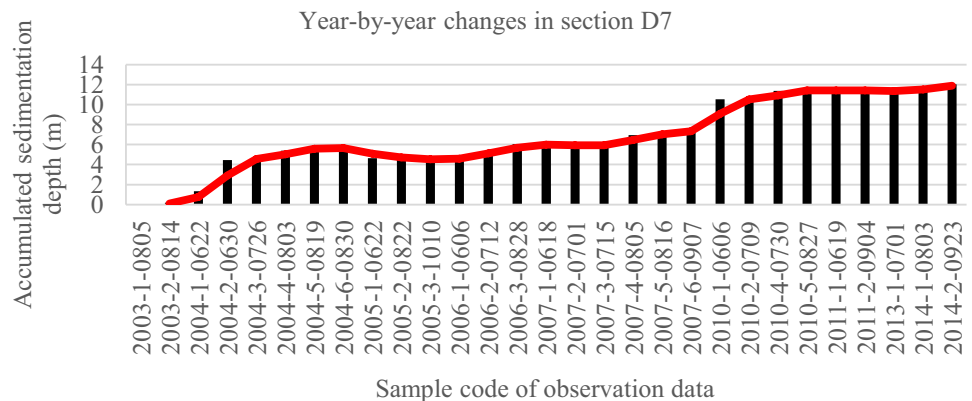


Fig. 4. This physical model was used to simulate the debris flow source region and the circulation and accumulation zones in the Jiangjia gully.

Descriptions and functions of the four main components/areas of the apparatus are as follows:

- The horizontal cross section of the materials' pool is a square with 1-m-long sides, a funnel-shaped bottom that allows the slurry to flow out, and a maximum capacity of 350 L. This pool holds the debris materials that were sieved to match the bulk densities of actual debris flows in the Jiangjia gully, and we refer to these as 'reconstructed debris flows' in this work. Once a reconstructed debris mixture is released, the materials'

pool acts as the source region for the simulated debris flows.

- The flow channel is 140-cm long, 30-cm wide, and 30-cm high. It slopes at a 30° angle and connects the gate of the materials' pool at the top and bottom, to the upstream edge of the trough, which simulates the gullies in the study area. The angle of the flow channel was chosen to give the reconstructed debris flows from the materials' pool a certain level of momentum and speed, enabling them to reach the 'debris flow gully' at the bottom.
- The rectangular simulated debris flow gully has two walls, both 73-cm high and 435-cm long, with a 70-cm distance between the walls. The slope of the simulated debris flow region was set to 5° in accordance with the

Fig. 4 Schematic diagram of the apparatus used to investigate the effects of the morphology of sediment-transporting channels on debris flow erosion and deposition. **a** Lateral view and **b** vertical view of the apparatus

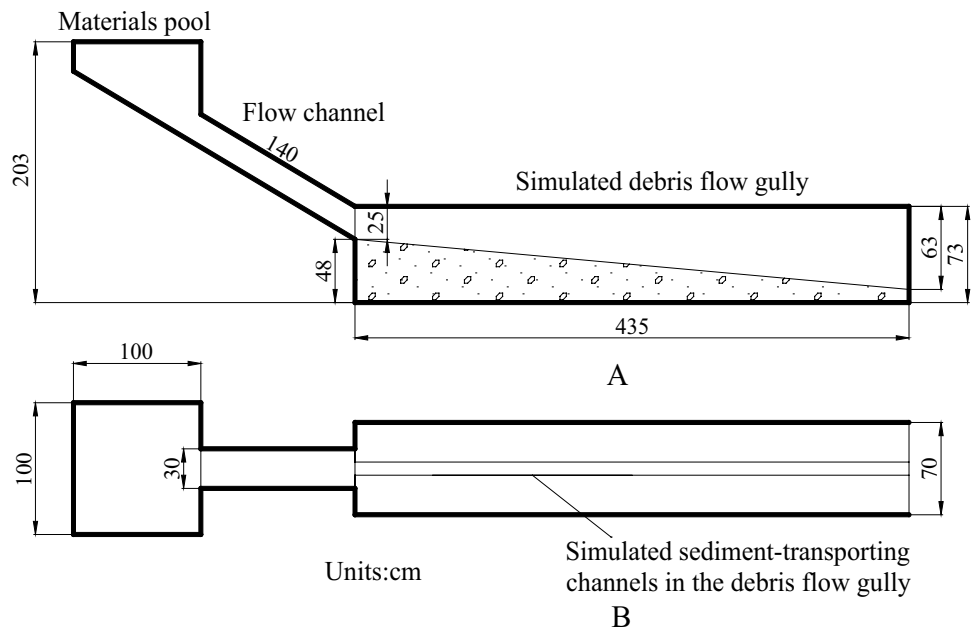


Table 1 More details about the explanation of the flume experiment

Grain size of the material (cm)	≤2
Bulk density (g/cm ³)	1.95
Number of cross sections	9
Times (run experiment)	3
Duration of each experiment (h)	1

actual gradient of the circulation zone in the Jiangjia gully.

- The excavated accumulation zone at the downstream end of the simulated circulation zone has a width of 3 m and a length of 5 m. A 3 × 6 m² sheet of colored cloth was placed in this zone to facilitate measurements of the simulated alluvial fans (debris flow lobes).

The debris flow materials/sediments used in the reconstructed debris flows and the simulated debris flow gully are debris flow deposits from the Jiangjia gully that were passed through a 2-cm sieve and have a bulk density of 1.95 g/cm³. More details are listed in Table 1.

Experimental content and procedures

Six types of sediment-transporting channel morphology and three sizes of debris flow were selected in accordance with the objectives of these experiments (Table 2). Prior to the start of each experiment, a channel of appropriate scale was excavated in the simulated debris flow gully, as shown in Fig. 5. Because it was difficult to excavate a channel

Table 2 Morphological parameters of sediment-transporting channels and debris flow sizes

Morphology of the channel cross section (cm ²) ^a	Sinuosity index of the channel	Total volume of the debris flow (L)
Even surface (no channel)	N/A	150
Even surface (no channel)	N/A	200
Even surface (no channel)	N/A	250
30 × 5	1	150
30 × 5	1	200
30 × 5	1	250
20 × 7.5	1	150
20 × 7.5	1	200
20 × 7.5	1	250
15 × 10	1	150
15 × 10	1	200
15 × 10	1	250
20 × 7.5	1.05	150
20 × 7.5	1.05	200
20 × 7.5	1.05	250
20 × 7.5	1.1	150
20 × 7.5	1.1	200
20 × 7.5	1.1	250

^aThe cross-sectional dimensions are presented as width × depth

with a rectangular cross section in the simulated circulation zone, owing to loose and dry sediments, 6 L of water were first sprayed onto the slope before each excavation to allow the sediment layers to consolidate and harden, after which the channel was excavated.

Fig. 5 Six channel morphologies set up for this experiment



Data acquisition and processing

Debris flow erosion and deposition experiments were performed with varying channel morphologies, and cross-sectional measurements were taken of the simulated debris flow gully after the end of each experiment. As the first 25 cm of the simulated circulation zone was strongly affected by the erosion of the flows, no measurements were performed on this section. Therefore, we started at 25 cm and measured nine segments, which consist of eight equidistant intervals (every 50 cm) and one interval of 10 cm. The depths of the debris flow deposits at each section were recorded. The areas and volumes of the deposits were calculated based on the measured depth, length, and width of the deposits. This process involved the following calculations:

Calculation of the sinuosity index (K_a) of the sediment-transporting channel: The sinuosity index (K_a) refers to the ratio between the actual length (L) and the straight-line length (the line connecting the two points, I) of the channel:

$$K_a = L/I. \quad (1)$$

Calculation of the deposit volumes in each section: for any given section, by first measuring the debris flow deposit depths at each of the above-mentioned points, the volume of every debris flow deposit between adjacent sections (having areas of S_i and S_{i+1}) can then be calculated. The formula for

calculating the volume of a prism is used to calculate the volume of a debris flow deposit between two sections:

$$V_{si} = d_i \left(S_{i+1} + S_i + \sqrt{|S_{i+1}S_i|} \right) / 3. \quad (2)$$

In this formula, S_i and S_{i+1} are the deposit sections (areas) of two neighboring sections, and d_i is the distance (in cm) between the two sections.

Results

Analysis of the erosion and deposition characteristics of channel-less regions of flow

With no channels present, we measured the lengths, widths, and heights (depths) of the depositional and erosional structures of three debris flows, each having a different total volume, at 0.5-m intervals. The magnitudes (volumes) of erosion/deposition at each of these intervals along the total travel distance were calculated and are shown in Fig. 6. Small- and medium-scale debris flows (150 and 200 L, respectively) did not easily reach the depositional zone, and the volumes of debris that did eventually reach the depositional zone were very small, even for large debris flows (250 L). Overall, the debris flows gradually slowed

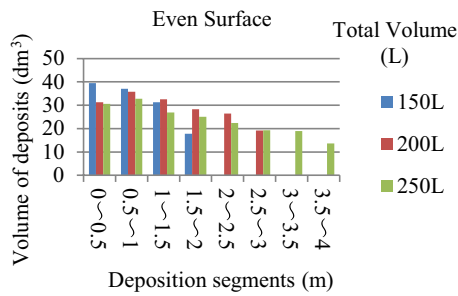


Fig. 6 Sectional debris flow deposits along the course of an even surface without a channel

down with travel distance and eventually stopped and settled. However, the depositional behavior varied for each flow. When the total volume of the debris flow was 150 L, a large quantity of the debris flow material was deposited close to the source; whereas as the travel distance increased, the quantity of deposited debris decreased and completely stopped around the midstream position. In contrast to the 150 L (small-scale) case, the deposited volumes of the 200 and 250-L debris flows did not decrease proportionally with travel distance but instead displayed smaller volumes of deposition closer to the source (0–0.5 m) compared to the next downstream section (0.5–1 m). The reason for this is that the quantities of materials and kinetic energies were highest at the start. The first 0.5-m (upstream) section was significantly affected by erosion, causing the deposits of debris flows from the source region to be transported via subsequent debris flows. As the travel distance increased, accretion of the subsequent surges created large deposits in the 0.5–1-m segment, resulting in the occurrence of peak debris deposition values within this interval. As the travel distance increased further (> 1 m), the amount of energy expended increased, and the total volume of the debris flow further decreased. The deposits decreased proportionally from this point, such that none of the debris flows reached the accumulation zone at the end of the simulated gully. This pattern of change, in which deposit volumes were relatively low at first then increased and subsequently decreased, did not occur for the 150-L (small-scale) debris flow under these slope conditions, as the kinetic energy possessed by the initial volume was not very large.

Erosional and depositional characteristics of straight channels

Debris flow erosion and deposition in the channels of the circulation zone were continuous processes. By fitting and analysis of the erosion and deposition magnitudes along the travel distance, a normal probability–probability (P–P) plot (Fig. 7) was used to verify that in straight channels, the pattern of deposition and erosion showed a normal distribution

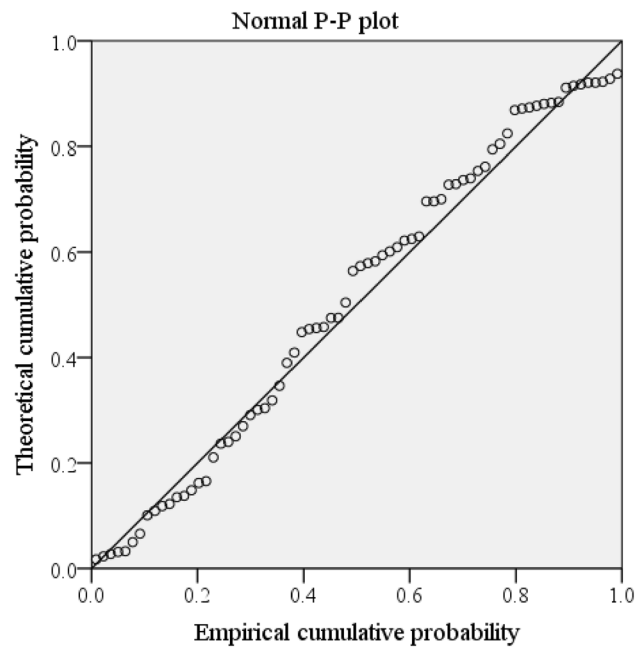
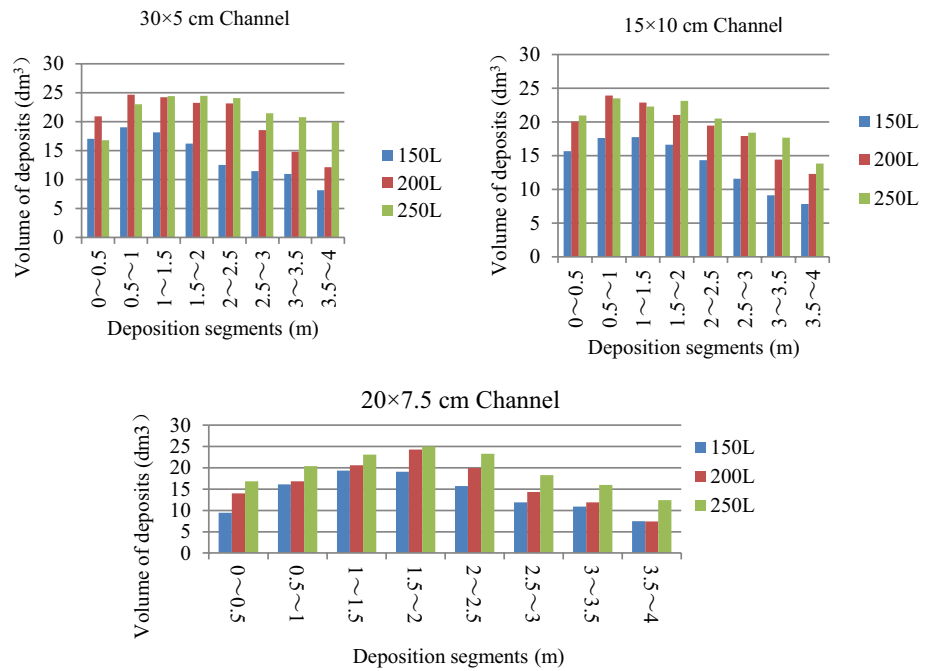


Fig. 7 Normal probability test of the quantity of erosion and deposition with respect to travel distance

with respect to travel distance (sample data points clustered close to the diagonal of the first quadrant). This pattern indicates that debris flow erosion and deposition in the circulation zone (especially deposition) can increase or decrease along the travel distance and that the peak value will appear, where deposition has occurred, with the deposit volumes progressively decreasing beyond this peak. We can divide the circulation zone into three segments, referred to as the upstream (< 1 m), midstream (1–3 m), and downstream (3–4 m) segments. Owing to the presence of a straight channel, the debris flows were able to pass through the upstream, midstream, and downstream regions of the circulation zone and reach the deposition zone, regardless of size. Through comparison, we found that without the presence of a channel the 150- and 200-L debris flows stopped in the circulation zone; whereas with a straight channel, the minimum and maximum volumes of deposition in the deposition zone were 14.64 and 51.24 L, respectively, with these values accounting for 10 and 25% of the total volume of the debris flow. In other words, the presence of a straight channel increased the runout of the debris flows by 10–25%. Furthermore, the presence of a straight channel caused all three sizes of debris flows to have depositional volumes that were low at first, then increased up to a peak value, and finally tapered off with respect to the travel distance (Fig. 8). The question arose as to why even 150-L debris flows displayed this pattern of deposition in the presence of a straight channel, unlike the deposition patterns shown by 150-L debris flows without a channel. This situation occurred, because

Fig. 8 Spatial variation in the debris flow deposits of three straight channels with different sectional morphologies



the presence of straight channels decreased the contact area between the debris flow and the gully bed, thus reducing the resistance caused by friction with the bed, which increased the travel distance of the debris flows in the circulation zone. For this reason, even for small-scale (150 L) debris flows, the quantity of debris flow deposition at the front end of a straight channel is less than that of an even surface without a channel. Accretion of the subsequent surges occurred naturally with the shift in travel distance, which caused the deposition peak to shift downstream. Subsequently, deposition in the straight channels was initially small, then increased up to a peak value, and finally decreased.

The cross-sectional areas of the three straight channels in this experiment (with widths and depths of 30×5 , 15×10 , and 20×7.5 cm^2) were all 150 cm^2 , and their respective hydraulic radii were 3.75, 4.29, and 4.29, as shown in Table 3. Differences in debris flow runout were found between each of these morphologies. In particular, the length and volume of the alluvial fan of the $30 \times 5\text{-cm}^2$

sediment-transporting channel were lower than those of the $15 \times 10\text{-}$ and $20 \times 7.5\text{-cm}^2$ channels. Hence, given the same cross-sectional area, the main factor that determines the runout of debris flows is the difference in hydraulic radius caused by differences in the width and depth of a channel. The greater the hydraulic radius, the greater the debris flow discharge in the circulation zone, which subsequently leads to larger alluvial fans at the mouth of the circulation zone.

Effect of sinuosity index on debris flow erosion and deposition

Differences were found between channels with sinuosity indices > 1 and straight channels regarding the distribution of debris flows with travel distance within the circulation zone. Analysis of the experimental data showed that, as the sinuosity index increases, the position of the deposition peak is shifted farther upstream (compared to that of straight channels or channels with very low sinuosity indices). For

Table 3 Debris flow deposition in three straight channels in the accumulation zone

Channel morphology (width \times depth)	150 L	200 L	250 L	Hydraulic radius
$30 \times 5 \text{ cm}^2$	Alluvial fan length 84 cm Approximate volume 14.64 dm^3	Alluvial fan length 104 cm Approximate volume 25.62 dm^3	Alluvial fan length 173 cm Approximate volume 62.22 dm^3	3.75
$15 \times 10 \text{ cm}^2$	Alluvial fan length 126 cm Approximate volume 21.96 dm^3	Alluvial fan length 162 cm Approximate volume 36.6 dm^3	Alluvial fan length 187 cm Approximate volume 69.54 dm^3	4.29
$20 \times 7.5 \text{ cm}^2$	Alluvial fan length 142 cm Approximate volume 29.28 dm^3	Alluvial fan length 163 cm Approximate volume 51.24 dm^3	Alluvial fan length 192 cm Approximate volume 73.2 dm^3	

straight channels (i.e., sinuosity index = 1), plotting the deposition volume for each interval against the travel distance indicates that all three sizes of debris flow have deposition peaks around the 2-m point (the midstream segment) along the travel distance (Fig. 8); whereas the deposition peaks for channels with a sinuosity index of 1.1 are all within a travel distance of 1 m (the upstream segment) (Fig. 9). Furthermore, as the sinuosity index increases, the resistance of the channel to debris flow movement increases significantly. For large-scale debris flows (250-L volume), when the sinuosity index increased from 1.05 to 1.1, the debris flow volume that reached the deposition zone decreased from 29.28 to 7.32 dm³. Without the presence of a channel, the volume of a 250-L debris flow that reached the deposition zone was 21.96 dm³ (Table 4). Hence, increases in the sinuosity index produced a greater degree of resistance to the movement of debris flows in the circulation zone compared to that produced by the dispersal of debris flow energy and volume on even surfaces without a channel. Furthermore,

comparing curved channels and straight channels, the maximum debris volume that reached the deposition zone was only 29.28 dm³ if curved channels were present, which is much lower than the 62.22-dm³ minimum recorded volume for straight channels.

This analysis shows that when bends are present along the channel, debris flows may display a super-elevation or run-up phenomenon. This causes a portion of the kinetic energy of the debris flow to be converted into potential energy following a super-elevation or run-up, thus expending the kinetic energy of the debris flow, while another portion of its energy may be depleted via collisions with the concave banks of the channel corners. This situation results in deceleration of the debris flow. Furthermore, this deceleration effect can cause smaller debris flows to stop and deposit sediments within the circulation zone through several stages of energy loss and deceleration, thus preventing these smaller flows from reaching the deposition zone downstream. Another cause for this result is that the curvature of curved channels increased the effective

Fig. 9 Spatial variations in debris flow deposition volumes in channels with different sinuosity indices

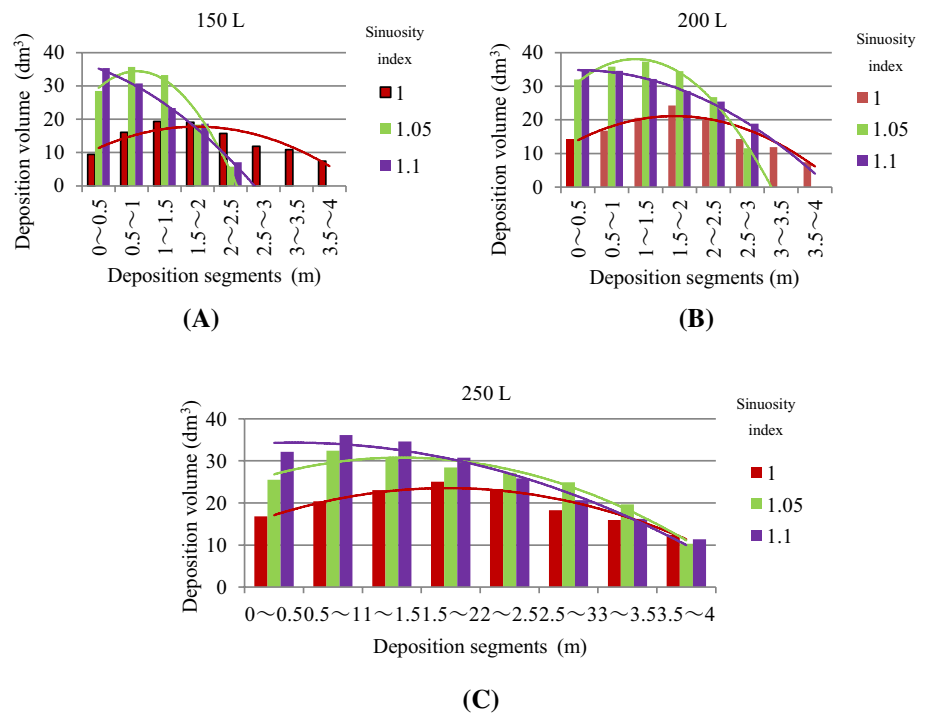


Table 4 Comparison between debris flow deposition on an even surface without a channel and with curved channels

Channel morphology (width × depth)	150 L	200 L	250 L
No channel present	Travel distance 205 cm No alluvial fan was formed	Travel distance 314 cm No alluvial fan was formed	Length of alluvial fan 133 cm Approximate volume 21.96 dm ³
20 × 7.5 cm ² (sinuosity index = 1.05)	Travel distance 249 cm No alluvial fan was formed	Travel distance 327 cm No alluvial fan was formed	Length of alluvial fan 152 cm Approximate volume 29.28 dm ³
20 × 7.5 cm ² (sinuosity index = 1.1)	Travel distance 242 cm No alluvial fan was formed	Travel distance 322 cm No alluvial fan was formed	Length of alluvial fan 87 cm Approximate volume 7.32 dm ³

length of the flow path, and if the difference in height between the two ends of the circulation zone remains unchanged, the hydraulic gradient of the debris flow is effectively decreased (i.e., the power provided by the debris flow per unit length is decreased). This effect, in addition to the effects of friction between the debris flow and the underlying surface, causes the debris flow to settle within the circulation zone.

Our experiments also showed that, with increases in the sinuosity index, the obstructive effects of the bending channel are manifest not only in terms of impact on the overall sizes of the deposits, but also on the volumes of debris flow deposits within unit intervals (0.5 m) of the circulation zone. However, this effect is not simply positively correlated with changes in the sinuosity index and is affected by the initial size of the debris flow. For medium-scale (200 L) and small-scale (150 L) debris flows, a sinuosity index of 1.05 results in a higher debris flow volume within each interval (0.5 m) and a more significant rate of decrease in deposit volumes beyond the depositional peak (with the gradients of the corresponding trend lines reflecting the degree of change), compared to the variations obtained with a sinuosity index of 1.1. This relationship is shown in Fig. 9a, b. For large-scale debris flows (250 L), as shown in Fig. 9c, the deposit volumes in the intervals corresponding to the midstream and upstream segments of the circulation zone (0–2.5 m) increase as the sinuosity index increases. However, the deposits in unit intervals of the downstream regions show stochastic behavior and do not show any significant correlation with the sinuosity index, which may be because of the substantially decreased energies and total volumes of the debris flows in this segment. Nonetheless, overall, the presence of curved channels significantly reduces the energies and quantities of debris flows, thus reducing their destructiveness, which contrasts sharply with the effect of straight channels in increasing debris flow discharges.

The data obtained from our simulations appear to indicate that debris flow erosion and deposition interact with channel morphologies. When debris flows act on curved channels, the banks of the channel recede due to erosion, while the convex banks advance because of deposition, which leads to a spring-like mode of development in these channels. The channel develops laterally in a swing-like manner while extending in the longitudinal direction along the bed of the circulation zone. This situation also results from the collective actions of lateral erosion on the gully banks and of erosional downcutting.

Discussion

Scientists have done many works to study the relationship between gully erosion and the controlling factors, and obtained some results. Poesen et al. (2003) summarised some statistical

data to show the contribution of gully erosion to overall soil loss rates and sediment production rates by water erosion, and the result indicated that soil loss rates by gully erosion represent from minimal 10 up to 94% of total sediment yield caused by water erosion. Though, the percentage of soil loss rates are similar to our experimental results, they emphasised the external factors of gully, like addressing the effects of spatial scale (size of study area) (Akgun et al. 2008; Chang and Chao 2006; Ranjan et al. 2004) and temporal scale (time span) and focusing on environmental factors (Baillie and Davies 2002; Best Heather 2002; Csiki and Rhoads 2014; Huisink et al. 2002).

Furthermore, we compared our present study with Li et al. (2015). Although we all explored the influence of channel morphologies on debris flow erosion and deposition, they focused more on the external characteristics of the channel including catchment size, elevation difference. Maybe, the correlation between external characteristics of channels and erosion (deposition) of debris flows in one area is generally different from other areas. Therefore, it is difficult to state how the morphology of channels affect the deposition or erosion of debris flow. Kean et al. (2013) pointed out one theory that the erosion of the channel was caused by the destruction of the channel-bed or the failure of the channel bank. In a word, the internal characteristics of the channel should not be ignored. In our study, we demonstrated the relationship between the sinuosity index and erosion and deposition of debris flow via flume experimentation. In the accumulation zone, the maximum deposition volume for a channel with a comparatively low sinuosity index (1.05) was > 50% of the minimum deposition volume for a straight channel. When the sinuosity index of the channel increased to 1.1, the circuitous route created by this curvature had a greater effect on debris flow deceleration and sedimentation than the diffusive effects of an even surface without channels. Comparing field observational data to experimental data, we realized the effects of channel morphology on the erosion and deposition of debris flow.

In addition, via the flume experiment, these findings are of significant importance for guiding debris flow risk assessment and for the restoration and reconstruction of downstream regions. Perhaps, combining the former studies focused on external characteristics of channel and our study focused on the internal characteristics of channel morphology could explain the influence of channel morphology on erosion and deposition more clearly. Following is an interesting phenomenon in the course of the experiment, and to some extent, it is not necessarily universal.

Characterization and comparison of debris flow deposit volumes and areas on the scale of deposits

We calculated the volumes and areas of debris flow deposits in the circulation zone by designating each 0.5-m region as a

deposition zone and fitting the changes in these quantities to travel distance. The resulting fitting relationships are shown in Tables 5 and 6. The fitting results demonstrate that the pattern of change in debris flow deposit volume within each deposition zone with respect to travel distance very closely fits a concave-downward parabolic shape, and that nearly, all the fits performed on the various sets of experimental results have correlation coefficients <0.9 (Table 5). This pattern of change is the same as that observed for the cross-sectional

areas of the debris flow deposits with respect to travel distance (Table 6); however, the latter displays significantly poorer fits, with a number of experimental results having correlation coefficients around 0.7 and 0.8 and >0.7.

Hence, differences in scale associated with the heights of deposits cannot be overlooked in terms of the variations in debris flow deposits with travel distance, and the impacts of deposit volumes must be taken into consideration in risk evaluations or in provision of early disaster warnings.

Table 5 Fitting relationships of the cross-sectional volume of the debris flow deposits (y) with respect to travel distance (x)

Shape of channel (cm ²)	Scale (L)	Fitting equation	R ²
No channels	150	$y = -11.112x^2 + 13.563x + 35.257$	0.997
	200	$y = -3.8092x^2 + 8.027x + 29.314$	0.9379
	250	$y = -0.3478x^2 - 3.5167x + 33.817$	0.9469
30 × 5	150	$y = -0.6202x^2 - 0.2164x + 18.639$	0.9128
	200	$y = -2.1255x^2 + 6.5241x + 19.084$	0.9569
	250	$y = -1.8941x^2 + 8.5629x + 14.679$	0.7486
15 × 10	150	$y = -1.2267x^2 + 2.7089x + 15.541$	0.946
	200	$y = -1.4297x^2 + 3.6159x + 19.968$	0.9357
	250	$y = -1.3249x^2 + 3.7423x + 20.06$	0.9415
20 × 7.5	150	$y = -2.9128x^2 + 11.542x + 6.3443$	0.8264
	200	$y = -3.5054x^2 + 13.537x + 8.0438$	0.8932
	250	$y = -2.9611x^2 + 11.683x + 12.006$	0.9312
20 × 7.5 (sinuosity index of 1.05)	150	$y = -4.0128x^2 - 2.2456x + 37.534$	0.9873
	200	$y = -9.4534x^2 + 25.523x + 20.848$	0.991
	250	$y = -3.373x^2 + 10.696x + 22.294$	0.9529
20 × 7.5 (sinuosity index of 1.1)	150	$y = -3.2044x^2 - 4.1056x + 38.033$	0.9901
	200	$y = -3.7713x^2 + 3.4771x + 35.909$	0.9963
	250	$y = -2.1936x^2 + 2.9294x + 33.35$	0.9679

Table 6 Fitting relationships of the cross-sectional area of the debris flow deposits (y) with respect to travel distance (x)

Shape of channel (cm ²)	Scale (L)	Fitting equation	R ²
No channels	150	$y = -223.75x^2 + 159.45x + 779.48$	0.9897
	200	$y = -92.332x^2 + 176.79x + 592.48$	0.8871
	250	$y = -24.254x^2 + 1.6654x + 595.9$	0.8009
30 × 5	150	$y = -20.975x^2 + 30.175x + 333.95$	0.7912
	200	$y = -43.797x^2 + 119.73x + 400.39$	0.8995
	250	$y = -42.676x^2 + 178.95x + 307.67$	0.7357
15 × 10	150	$y = -7.0104x^2 - 29.105x + 342.4$	0.9202
	200	$y = -21.333x^2 + 44.577x + 397.84$	0.8454
	250	$y = -46.499x^2 + 154.6x + 338.25$	0.6649
20 × 7.5	150	$y = -253.4x^2 + 435.91x + 493.31$	0.8601
	200	$y = -61.017x^2 + 201.24x + 253.78$	0.7525
	250	$y = -54.536x^2 + 186.43x + 311.02$	0.8597
20 × 7.5 (sinuosity index of 1.05)	150	$y = -253.4x^2 + 435.91x + 493.31$	0.8601
	200	$y = -101.64x^2 + 180.42x + 641.28$	0.8713
	250	$y = -79.752x^2 + 236.44x + 450.07$	0.9063
20 × 7.5 (sinuosity index of 1.1)	150	$y = -0.0023x^2 + 2.9779x - 342.39$	0.6814
	200	$y = -53.608x^2 + 35.65x + 689.84$	0.9895
	250	$y = -48.025x^2 + 65.437x + 645.72$	0.9402

Ideas for further investigations into the effects of channel morphology on debris flow erosion and deposition

We summarized the interactions between sediment-transporting channels with varying morphologies and debris flow erosion and deposition and compared the erosion and deposition in curved channels, straight channels, and even surfaces without channels. We found that the presence of straight channels can enhance the runout of debris flows and that differences in hydraulic radius associated with different channel widths and depths (with the same cross-sectional area for the sediment-transporting channel) are the primary factors determining the discharge capacity of debris flows. The findings of this study thus provide a reference for investigations into the movement patterns of debris flows. However, in this work, we only compared the above effects in terms of the scale of deposits. In follow-up studies on the effects of curved channels on debris flow erosion and deposition, the debris flow water content and impact pressure of the corners of a channel may be measured and calculated to enable analyses of the differences between curved and straight channels from the perspectives of soil and fluid mechanics. In reality, a cross section within the circulation zone may not be restricted to a single channel or even a single type of channel. Hence, detailed studies on the effects of channel morphology on debris flow erosion and deposition within the circulation zone should also include analyses of the erosion and deposition characteristics in cross sections with various channel combinations. Computational simulations may be used to perform the analyses of these combinations. Furthermore, erosion and deposition are affected by debris flow properties, in addition to the morphology of the channels. Hence, the erosional and depositional characteristics associated with different channel morphologies and with different bulk densities should also be taken into consideration.

Conclusions

In this work, flume experiments were performed to investigate the effects of channels in circulation zone of gully debris flows during depositional and erosional processes with six channel morphologies and three scales of debris flow. The results indicate that straight channels (compared with even surface) has increased 10–25% of the discharge capacity, and outrun is positively correlated with the hydraulic radius. In addition, straight channel helped debris flow deposits to be distributed normally with respect to travel distance. Besides, depositional peak also migrated farther downstream than in the presence of even surfaces without channels.

With regard to curved channels with low gradient, a slight increase in sinuosity index would result in prominent obstruction or blockage. In accumulation zone, the maximum deposition volume of curved channels with low sinuosity index (1.05) was > 50% of the minimum volume of straight ones. Furthermore, the curvature affected not only the depositional peak, but also debris flow deposition's quantity in each of the unit intervals. Furthermore, through comparison, the fitting between volume and travel distance showed a higher goodness of fit (correlation coefficients > 0.9) than area and travel distance. Therefore, the effects associated with differences in deposit volumes should be considered more carefully for risk evaluations and disaster safeguard purpose. In a word, the impacts of channel morphology on debris flows should not be overlooked, because it is highly significant for debris flow disaster prevention and disaster relief.

Acknowledgements This work was supported by the National Natural Science Foundation of China (Grant No. 41790434), the National Key Technology R&D Program (2014BAL05B01), and the National Natural Science Foundation of China (Grant No. 41471010). We are also grateful for the comments and criticisms of an early version of this manuscript by our colleagues and the journal's reviewers.

References

- Adhikari DP, Koshimizu S (2005) Debris flow disaster at Larcha, upper Bhotekoshi Valley: central Nepal. *Isl Arc* 14(4):410–423
- Akgun A, Dag S, Bulut F (2008) Landslide susceptibility mapping for a landslide-prone area (Findikli, NE of Turkey) by likelihood frequency ratio and weighted linear combination models. *Environ Geol* 54:1127–1143
- Baillie B, Davies T (2002) Influence of large woody debris on channel morphology in native forest and pine plantation streams in the nelson region, New Zealand. *N Z J Mar Freshw* 36(4):763–774
- Benda LE (1990) The influence of debris flow on channels and valley floors in the Oregon Coast Range, USA. *Earth Surf Process* 15(5):457–466
- Best Heather R (2002) The influence of ice on channel morphology of the Kuparuk River, Alaska. Boise State University theses and dissertations. 403. <https://scholarworks.boisestate.edu/td/403>
- Bocco G (1991) Gully erosion: processes and models. *Prog Phys Geogr* 15(4):392–406
- Bridge JS (2003) Rivers and floodplains: forms, processes, and sedimentary record. *Aust Geogr Stud* 2003 48(3):386–387
- Cannon SH, Gartner JE, Rupert MG, Rea MJA, Parrett AH C (2010) Predicting the probability and volume of postwildfire debris flows in the intermountain western united states. *Geol Soc Am Bull* 122:127–144
- Capra A, Porto P, Scicolone B (2009) Relationships between rainfall characteristics and ephemeral gully erosion in a cultivated catchment in Sicily (Italy). *Soil Tillage Res* 105(1):77–87
- Carnicelli S, Benvenuti M, Ferrari G, Sagri M (2009) Dynamics and driving factors of late Holocene gullying in the Main Ethiopian Rift (MER). *Geomorphology* 103(4):541–554
- Catani F, Casagli N, Ermimi L, Righini G, Menduni G (2005) Landslide hazard and risk mapping at catchment scale in the Arno Riverbasin. *Landslides* 2:329–342

- Chang S (2016) Research on scouring and deposition features and impact factors of gully debris flow—a case study on Jiangjia Gully, Yunnan Province, Thesis PhD, Institute of Mountain Hazards and Environment, Chinese Academy of Sciences, Chengdu (in Chinese)
- Chang TC, Chao RJ (2006) Application of back-propagation networks in debris flow prediction. *Eng Geol* 85:270–280
- Csiki SJ, Rhoads BL (2014) Influence of four run-of-river dams on channel morphology and sediment characteristics in Illinois, USA. *Geomorphology* 206(1):215–229
- Dotterweich M, Rodzik J, Zglobicki W, Schmitt A, Schmidtchen G, Bork HR (2012) High resolution gully erosion and sedimentation processes, and land use changes since the Bronze Age and future trajectories in the Kazimierz Dolny area (Nałęczów Plateau, SE-Poland). *Catena* 95:50–62
- Gregoretti C, Fontana GD (2008) The triggering of debris flow due to channel-bed failure in some alpine headwater basins of the Dolomites: analyses of critical runoff. *Hydrol Process* 22(13):2248–2263
- He Y (2003) Influence of debris flow on river channel change of mountains. Ph.D. Thesis, Institute of Mountain Hazards and Environment, Chinese Academy of Sciences, Chengdu (in Chinese)
- He ST, Wang DJ, Chen S, Zhang SJ, Chang SQ (2016) Natural consolidation characteristics of viscous debris flow deposition. *J Mt Sci* 13(10):1723–1734
- Hong Y, Wang JP, Li DQ, Cao ZJ, Ng CWW, Cui P (2015) Statistical and probabilistic analyses of impact pressure and discharge of debris flow from 139 events during 1961 and 2000 at Jiangjia Ravine, China. *Eng Geol* 187:122–134
- Huisink M, Moor JJWD, Kasse C, Virtanen T (2002) Factors influencing periglacial fluvial morphology in the northern European Russian tundra and taiga. *Earth Surf Process* 27(11):1223–1235
- Jing K (1986) A study on gully erosion on the Loess Plateau. *Sci Geogr Sin* 6(4):340–347 (in Chinese)
- Kean JW, McCoy SW, Tucker GE, Staley DM, Coe JA (2013) Run-off-generated debris flows: observations and modeling of surge initiation, magnitude, and frequency. *J Geophys Res Earth Surf* 118:2190–2207
- Kirkby MJ, Bracken LJ (2009) Gully processes and gully dynamics. *Earth Surf Process* 34(14):1841–1851
- Lan HX, Zhou CH, Wang LJ, Zhang HY, Li RH (2004) Landslide hazard spatial analysis and prediction using GIS in the Xiaojiang watershed, Yunnan, China. *Eng Geol* 76:109–128
- Lee S, Pradhan B (2007) Landslide hazard mapping at Selangor, Malaysia using frequency ratio and logistic regression models. *Landslides* 4:33–41
- Li X, Chen Q, Kang Z (1979) A preliminary analysis of the development process of the Jiangjiagou mudslides. *J Geog Sci* 2(156–168):185–186 (in Chinese)
- Li Y, Hu K, Chen X (2004) Thickness distribution of debris-flow deposition. *J Mater Sci* 3:332–336 (in Chinese with English abstract)
- Li L, Yu B, Zhu Y, Chu S, Wu Y (2015) Topographical factors in the formation of gully-type debris flows in Longxi River catchment, Sichuan, China. *Environ Earth Sci* 73(8):4385–4398
- Liu C, Dong J, Peng Y, Huang H (2009) Effects of strong groundmotion on the susceptibility of gully type debris flows. *Eng Geol* 104:241–253
- Major JJ (1997) Depositional processes in large-scale debris-flow experiments. *J Geol* 105(3):345–366
- Morgan RPC, Mngomezulu D (2003) Threshold conditions for initiation of valley-side gullies in the Middle Veld of Swaziland. *Catena* 50(2):401–414
- Pan HL, Wei LQ, Yang S, Ou GQ (2012) Evolution laws on longitudinal slope of gully affected by debris flow erosion. *Appl Mech Mater* 204–208:235–240
- Patton PC, Schumm SA (1975) Gully erosion, Northwestern Colorado: a threshold phenomenon. *Cancer Res* 44(7):3040–3050
- Poesen J, Nachtergaele J, Verstraeten G, Valentin C (2003) Gully erosion and environmental change: importance and research needs. *Catena* 50(2):91–133
- Prosser IP (1996) Thresholds of channel initiation in historical and Holocene times, southeastern Australia. *Q J Eng Geol* 16:1–11
- Ranjan KD, Shuichi H, Atsuko N, Minoru Y, Takuro M, Katsuhiko N (2004) GIS-based weights-of-evidence modelling of rainfall induced landslides in small catchments for landslide susceptibility mapping. *Environ Geol* 54:311–324
- Rengers FK, Tucker GE (2014) Analysis and modeling of gully headcut dynamics, North American high plains. *J Geophys Res Earth* 119(5):983–1003
- Rengers FK, Tucker GE (2015) The evolution of gully headcut morphology: a case study using terrestrial laser scanning and hydrological monitoring. *Earth Surf Process* 40(10):1304–1317
- Rozos D, Skilodimou HD, Loupasakis C, Bathrellos GD (2013) Application of the revised universal soil loss equation model on landslide prevention. An example from N. Euboea (Evia) Island, Greece. *Environ Earth Sci* 70(7):3255–3266
- Soil Science Society of America (2001) Glossary of soil science terms. Soil Science Society of America, Madison. <http://www.soils.org/sssagloss/>
- Tiranti D, Bonetto S, Mandrone G (2008) Quantitative basin characterisation to refine debris-flow triggering criteria and processes: an example from the Italian Western Alps. *Landslides* 5:45–57
- Tunusluoglu MC, Gokceoglu C, Nefeslioglu HA, Sonmez H (2008) Extraction of potential debris source areas by logistic regression technique: a case study from Barla, Besparmak and Kapi mountains (NW Taurids, Turkey). *Environ Geol* 54:9–22
- Valentin C, Poesen J, Li Y (2005) Gully erosion: impacts, factors and control. *Catena* 63(2):132–153
- Vandekerckhove L, Poesen J, Wijdenes DO, Gyssels G, Beuselinck L, Luna ED (2000) Characteristics and controlling factors of bank gullies in two semi-arid mediterranean environments. *Geomorphology* 33(1):37–58
- Vanwallegem T, Bork HR, Poesen J, Schmidtchen G, Dotterweich M, Nachtergaele J (2005) Rapid development and infilling of a buried gully under cropland, central Belgium. *Catena* 63(2):221–243
- Wells RR, Bennett SJ, Alonso CV (2009) Effect of soil texture, tailwater height, and pore-water pressure on the morphodynamics of migrating headcuts in upland concentrated flows. *Earth Surf Process* 34(14):1867–1877
- Wenske D, Jen CH, Böse M, Lin JC (2012) Assessment of sediment delivery from successive erosion on stream-coupled hillslopes via a time series of topographic surveys in the central high mountain range of Taiwan. *Quatern Int* 263:14–25
- Wu J, Kang Z, Tian L (1990) Observational study on the debris flow in Jiangjiagou, Yunnan Province. Science Press, Beijing, pp 1–3 (in Chinese)
- Xiong D, Yan D, Yi L, Lu X, Han J, Han X (2010) Simulation of morphological development of soil cracks in Yuanmou Dry-hot Valley region, Southwest China. *Chin Geogr Sci* 20(2):112–122
- You Y, Cheng Z (2005) The influence of discontinuous motion of viscous debris flow on erosion and deposition of Gully bed-study of the case at Jiangjia Gully in Dongchuan, Yunnan. *J Disaster Prev Mitig Eng* 02:146–151 (in Chinese)
- Zhu TX (2012) Gully and tunnel erosion in the hilly Loess Plateau region, China. *Geomorphology* 153:144–155